

# Submicron Etched Beam Splitters Based on Total Internal Reflection in GaAs/AlGaAs Waveguides

Byungchae Kim and Nadir Dagli *Fellow, IEEE*

**Abstract**— Submicron etched beam splitters are designed, fabricated and characterized in  $\text{Al}_{0.9}\text{Ga}_{0.1}\text{As}/\text{GaAs}$  waveguides. Beam splitter transmission and reflection characteristics show clear dependence on gap dimension and angle of incidence. It is possible to obtain 8 to 30% power transmission by adjusting the gap dimension and angle of incidence. The experimental results agree well with three-dimensional (3D) finite difference time domain (FDTD) simulations. The effect of imperfections, mainly the slope of etched sidewalls and variations in etch depth are investigated using 3D FDTD. Design guidelines for low loss etched beam splitters are also given.

**Index Terms**— Total internal reflection, beam splitter, weakly confined waveguide, integrated optics.

## I. INTRODUCTION

Weakly-guiding conventional waveguides are widely used in most mature photonic components because they have low scattering loss and can be optimized for effective optical gain using well established regrowth techniques. But large scale integration of components utilizing such waveguides is difficult due to lack of sharp bends, compact splitters and couplers. This is mainly due to high radiation loss of waveguide bends with small radius of curvature and long coupling length of couplers for appreciable amount of coupling. Long couplers and large radius bends occupy very large areas which increase the chip size. This in turn increases cost and creates uniformity issues.

One solution to this problem is to use mirrors based on total internal reflection (TIR) and couplers based on etched beam splitters (EBS). TIR mirror was successfully demonstrated and used for sharp waveguide bends [1]-[8]. EBS can also be a promising candidate for compact couplers or beam splitters [12]. A deeply etched narrow trench can be used just like a bulk optic beam splitter and power splitting ratio can be easily modified by changing device geometry. Furthermore, the fabrication process of EBS is the same as that of TIR mirror. In a photonic circuit based on weakly guiding waveguides

fabrication of these components usually require one additional process step which is deep etching. Therefore integration of EBS and TIR mirror into a weakly guiding platform is straightforward. Hence such EBS and TIR mirrors can be basic building blocks and reduce entire device size in photonic integrated circuits. For example, compact resonators using EBS, TIR mirrors and conventional waveguides are recently demonstrated [9]-[12]. In this paper, Benzocyclobutane (BCB)-filled EBS in  $\text{Al}_{0.9}\text{Ga}_{0.1}\text{As}/\text{GaAs}$  material system is designed fabricated and characterized. The measured characteristics are compared with both 2D and 3D FDTD simulation. The effect of fabrication errors on EBS characteristics is investigated using 3D FDTD simulation. Finally guidelines for low loss EBS design are outlined

## II. DEVICE DESCRIPTION AND SIMULATION

EBS is formed by etching a narrow trench across a waveguide as schematically illustrated in Figure 1 (a). When TIR occurs, an evanescent field exists in the lower index etched gap region. If a transmission waveguide on the other side of the etched trench is placed close enough so that the evanescent field does not vanish at the interface of the transmission waveguide, certain amount of incident power can be coupled to the transmission waveguide. The reflected power at the deeply etched interface can be captured by another waveguide, called the reflection waveguide. The power splitting ratio between transmission and reflection waveguides depends on the angle of incidence, the dimensions of the gap and the index of refraction of the lower index material in the gap. In this work the waveguides used are 2  $\mu\text{m}$  wide rib waveguides etched 0.65  $\mu\text{m}$  deep into an  $\text{Al}_{0.9}\text{Ga}_{0.1}\text{As}/\text{GaAs}$  epilayer as shown in Figure 1 (b). The epilayer is grown by MBE and has two 0.75  $\mu\text{m}$  thick  $\text{Al}_{0.9}\text{Ga}_{0.1}\text{As}$  claddings and a 0.44  $\mu\text{m}$  thick GaAs core. It also has a 0.02  $\mu\text{m}$  GaAs top layer and is unintentionally doped.

In the initial design two-dimensional 2D FDTD method is used to numerically simulate the proposed structure. 2D FDTD requires far less memory and computational resources compared to 3D FDTD. Hence it is possible to generate design trends quickly with 2D FDTD. For 2D FDTD analysis 3D waveguide is reduced to 2D using effective index method. The calculated refractive indices of core and cladding regions of the 2D equivalent waveguide are 3.219 and 3.207, respectively.

Manuscript received February 5, 2010. This work was supported by Office of Naval Research through Naval Postgraduate School. Authors are with the Electrical and Computer Engineering Department, University of California, Santa Barbara, CA 93106.

Copyright (c) 2009 IEEE. Personal use of this material is permitted. However, permission to use this material for any other purposes must be obtained from the IEEE by sending a request to pubs-permissions@ieee.org.

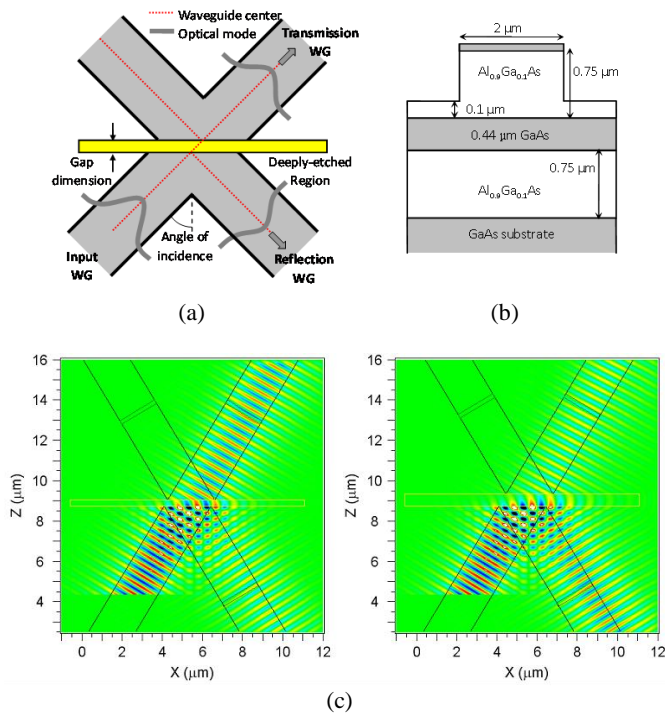
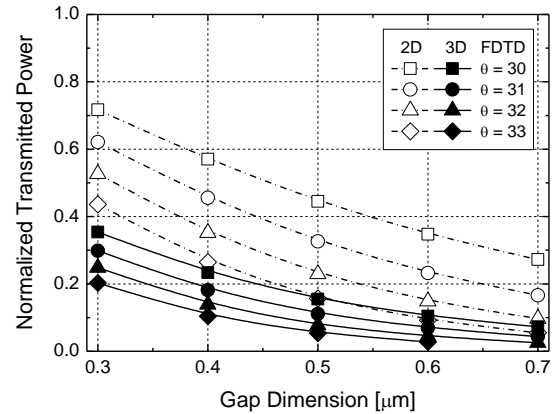


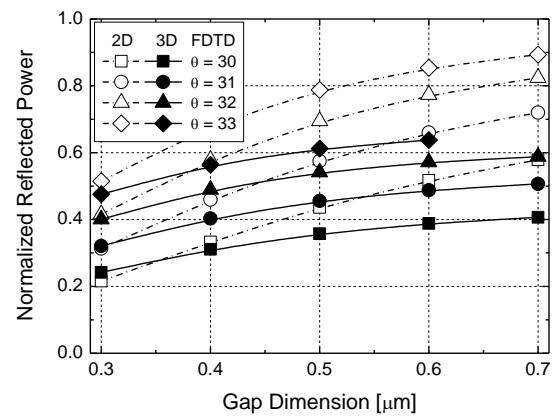
Figure 1. (a) Top schematic of the etched beam splitter, (b) waveguide cross sectional profile, and (c) magnetic field intensity ( $H_y$ ) for gap dimension of 0.3  $\mu\text{m}$  (left) and 0.6  $\mu\text{m}$  (right) when angle of incidence is 31°.

In our design, the etched gap is filled with BCB (CYCLOTENE 3022-46) to increase the critical angle so that larger angles of incidence can be used for appreciable transmission. The refractive index of BCB is 1.534 around 1.55  $\mu\text{m}$  and correspondent critical angle is around 28°. This is about 10° larger than the air trench case. The increase in the critical angle helps to reduce device size utilizing EBS. In the calculations the fundamental TM mode of the 2D equivalent waveguide, which corresponds to the fundamental TE of the actual waveguide, is used as the input excitation at  $\lambda = 1.55 \mu\text{m}$  for the given structure. The mesh size in x- and z-direction is 0.005  $\mu\text{m}$  and the time step is  $\sim 0.67 \times 10^{-17}$  s. To minimize numerical error during mesh generation, the trench section is aligned with one of the coordinate axes.

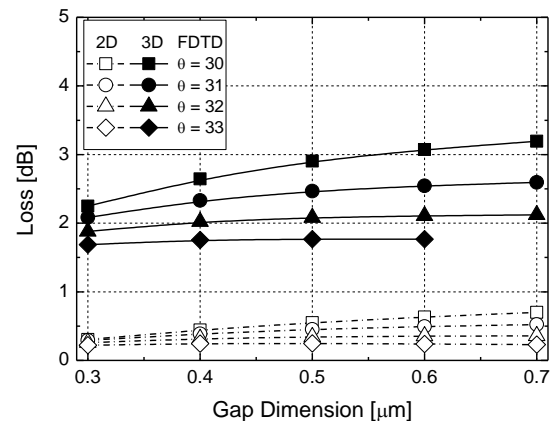
Figure 1 (c) shows magnetic field intensity,  $|H_y|$ , for gap dimension of 0.3 and 0.6  $\mu\text{m}$ , respectively, when angle of incidence is 31°. There is more coupling and less reflection as gap gets narrower. It is also observed that the center of the transmitted and reflected optical mode slightly deviates from waveguide center. Since reflection is based on TIR, reflection coefficient has a certain phase, which is due to the penetration of the fields into the gap. This manifests itself as a lateral shift of the reflected beam along the interface. The transmission beam center deviates from the center of the input waveguide due to propagation along the etched facet in the lower index gap region. Therefore, positions of both reflection and transmission waveguides should be optimized to minimize EBS loss for a given gap dimension and angle of incidence. The required alignment accuracy of the waveguide centers with respect to gap is usually sub micron. This can be achieved using a self aligned process.



(a)



(b)



(c)

Figure 2. Comparison between 2D and 3D FDTD simulation: (a) normalized power transmission, (b) reflection, and (c) loss of etched beam splitter as a function of gap dimension for different angles of incidence. In 2D FDTD, the fundamental TM mode of the 2D equivalent waveguide is used as the input excitation at  $\lambda = 1.55 \mu\text{m}$ . The fundamental TE mode is used as the input excitation at  $\lambda = 1.55 \mu\text{m}$  for 3D FDTD. Open symbols are the 2D FDTD results and connected closed symbols are the 3D FDTD results.

In Figure 2 (a) and (b), normalized power transmission and reflection from 2D FDTD are plotted as function of gap dimension for different angles of incidence using open symbols.

As gap dimension increases, transmission decreases while reflection correspondingly increases. For a given gap dimension, transmission decreases and reflection increases as angle of incidence increases. This is understandable because the evanescent field decreases more rapidly in the lower index region when angle of incidence increases. As shown in Figure 2 (c), EBS loss increases as gap dimension increases for a given angle of incidence. As incident angle increases, loss decreases and also gap dependence becomes smaller. When angle of incidence is  $33^\circ$ , EBS loss is less than 0.4 dB for all considered gap dimensions. This can be understood considering the plane wave spectrum of the mode. Not all the plane wave components in this spectrum experience TIR. Part of these components experience multiple reflections in the gap and are not effectively collected by the reflection and transmission waveguides. This contributes to the loss. Increasing angle of incidence assures that most of the plane wave components in the mode spectrum experience TIR and loss decreases.

To predict more accurate results, same EBS structures are simulated with three-dimensional (3D) FDTD method. In 3D FDTD simulation, the mesh size is  $0.02 \mu\text{m}$  in both x- and z-direction and  $0.04 \mu\text{m}$  in vertical direction (y-direction). The time step is  $3.3 \times 10^{-17}$  s. 3D simulation results are plotted using connected closed symbols in Figure 2. While the trends in transmission and reflection as a function of gap and angle of incidence agree well with the predicted with 2D FDTD simulation, the absolute values of both coefficients are less. For example when angle of incidence is  $32^\circ$ , for gap dimension between 0.3 and  $0.6 \mu\text{m}$ , the transmission is 5 to 25% in 3D FDTD while 2D FDTD simulations estimate power transmission of 15 to 52%. There is a similar reduction in reflection. These reductions both in reflection and transmission mean that the loss is higher. Based on these simulations, the effect of confinement or the plane wave spectral width in vertical direction should be considered in EBS design. However 3D simulation requires much more simulation time and memory. Hence even though 2D simulation overestimates EBS characteristics, it can be still used during optimization process to determine trends due to its computational efficiency. Since 2D characteristics are better making the problem more 2D like, by making vertical confinement even weaker should help to improve EBS characteristics. This of course requires deeper etching which could be difficult especially for narrow gaps.

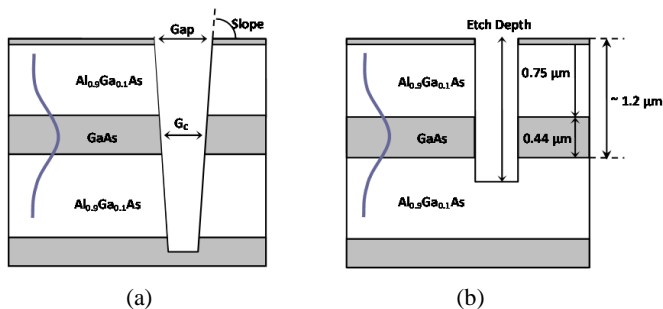


Figure 3. (a) EBS cross section when the etch profile is not vertical. This changes the actual gap dimension at center of waveguide core, and (b) EBS with insufficient etch depth. The required etch depth is  $2.2 \mu\text{m}$  to guarantee that entire optical mode experiences TIR.

The effect of possible non idealities in the fabrication is also considered with 3D FDTD. The most likely candidates are the non vertical sidewalls and insufficient etch depth of the etched gap as shown in Figure 3. The non vertical gap profile is commonly observed in high aspect-ratio etching. When dimension of the gap top is fixed as illustrated in Figure 3(a) an inclined facet results and the gap dimension changes. A calculation showing the effect of gap slope on EBS characteristics is shown in Figure 4.

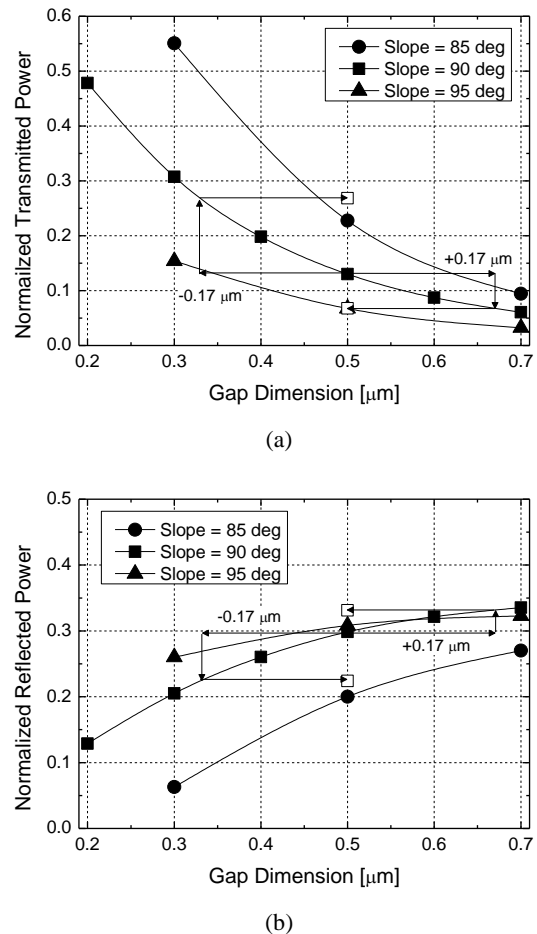
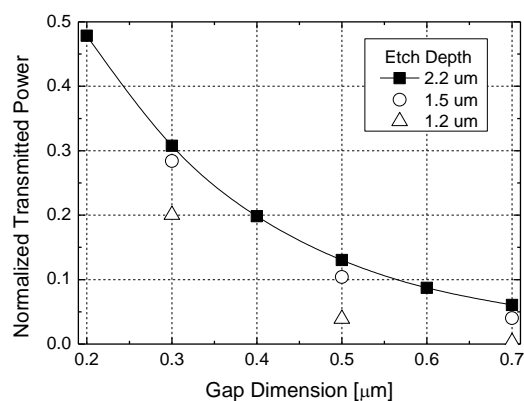
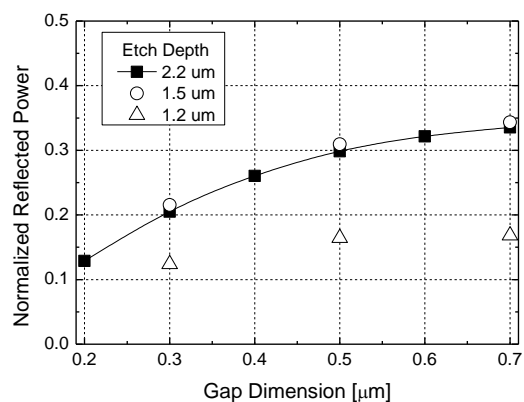


Figure 4. Effects of non vertical etch profile on EBS (a) transmission and (b) reflection based on 3D FDTD calculations. A sidewall slope of  $\pm 5^\circ$  corresponds to  $\mp 0.17 \mu\text{m}$  change in gap dimension at the center of the waveguide core. The transmission/reflection of the sloped sidewall EBS is almost identical to that an ideal EBS with a  $\mp 0.17 \mu\text{m}$  different gap as indicated by the arrows.

When slope is  $85^\circ$ , transmission increases while reflection decreases. This trend is mainly due to reduced gap dimension at center of waveguide core. In this case this reduction is  $0.17 \mu\text{m}$ . If we consider an ideal trench with vertical sidewalls in which the gap is reduced  $0.17 \mu\text{m}$ , the calculated reflection and transmission are very close to the calculation with  $85^\circ$  sidewall slope as indicated in Figure 4. Insufficient gap depth, as illustrated in Figure 3 (b), is the other imperfection considered. This is possible especially for narrower gap dimension due to high aspect ratio.



(a)



(b)

Figure 5. Effect of trench depth on EBS (a) transmission and (b) reflection. If the trench is not deep enough there is significant reduction in both transmission and reflection.

Figure 5 shows the effect of etch depth on EBS characteristics. As etch depth decreases, both transmission and reflection generally decreases. If gap is not deep enough some portion of mode cannot experience TIR and experiences a non uniform index discontinuity which creates scattering. Based on 3D FDTD if the etch clears the bottom of the waveguide core by about  $0.30 \mu\text{m}$  the degradation is negligible. This is almost as deep as the extent of the optical mode below the core. If the etch extends only to the bottom of the core, i.e.,  $1.2 \mu\text{m}$ , degradation is significant.

The roughness of etched EBS interface also contributes to the loss. The effect of this roughness can be discussed considering the Fourier transform of the surface roughness. Low spatial components effectively create a tilt of the interface and are the most troublesome. The source of these components is typically the alignment inaccuracy. This problem can be eliminated using a self aligned process. Higher spatial frequency components create scattering, but their amplitudes are typically lower. We estimate the loss due to these components by comparing the experimentally obtained lowest TIR mirror loss with FDTD simulations. This loss, which is attributed to high frequency roughness of the interface, is about 0.2 dB.

EBS has polarization dependent characteristics. In FDTD

simulations, TM mode reflects more and transmits less. Furthermore optimum interface position is different for both polarizations and it is not possible to use the same EBS for both polarizations. But in practice this is not a problem since the other integrated optical elements considered, namely waveguides, TIR mirrors, and devices made out of them have also polarization dependent characteristics. All the results given in this paper are for TE polarization.

### III. FABRICATION AND CHARACTERIZATION

The top schematic of fabricated EBS is shown in Figure 6. Two TIR mirrors are used to direct the reflected light at EBS such that convenient measurements using cleaved facets can be made. In fabrication process, a self-aligned process is used to reduce additional loss caused by misalignment between waveguides and etched facets.

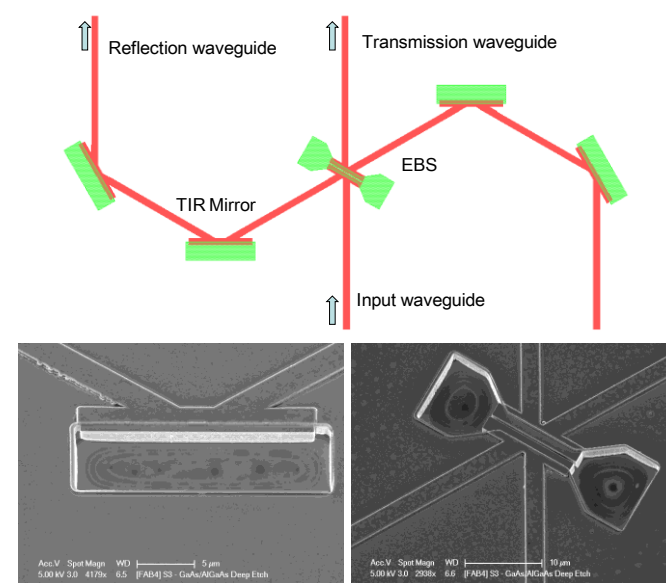
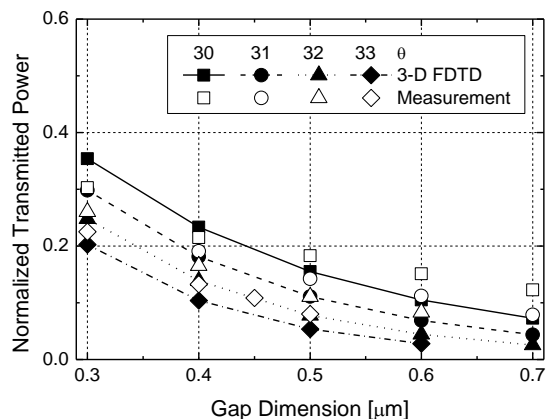


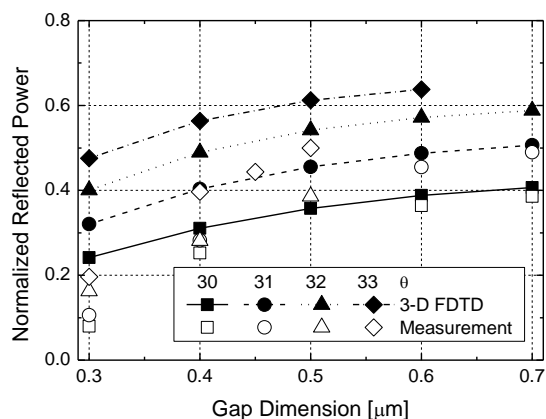
Figure 6. Top schematic of fabricated etched beam splitter with 2 TIR output mirrors for changing propagation direction. SEM images of etched beam splitter and TIR mirror before filling trenches with BCB are also shown.

First, all patterns including waveguides, EBS and TIR mirrors are defined using electron beam lithography. Then,  $100\text{\AA}$  titanium and  $1500\text{\AA}$  nickel are evaporated and lifted off to form the etch mask. This mask is used to etch the waveguides, EBS and TIR mirrors in two etch steps. Since entire device is defined by the same mask, the precise alignment between waveguides and mirror facets is guaranteed. Next, the EBS and TIR mirror patterns are covered by photoresist to avoid unnecessary damage to the etch mask during waveguide etching. The upper cladding layer ( $\text{Al}_{0.9}\text{Ga}_{0.1}\text{As}$ ) is etched to a depth of  $0.65 \mu\text{m}$  to form the waveguide using the reactive ion etching (RIE) with  $\text{BCl}_3:\text{SiCl}_4$ . The etch depth is precisely controlled with laser monitoring to guarantee the single mode operation. After waveguides are etched,  $4000 \text{\AA}$   $\text{SiO}_2$  film is deposited over the entire sample by plasma enhanced chemical vapor deposition (PECVD) and areas which will be deeply etched were opened using standard photolithography. This exposes the original mask. This is followed by deep gap etching

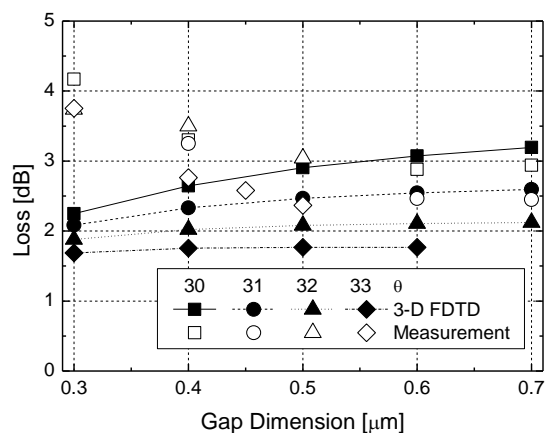
using inductively coupled plasma (ICP) RIE with  $\text{BCl}_3$ :  $\text{Cl}_2$ : Ar. SEM pictures of fabricated TIR mirror and EBS before BCB-filling are shown in Figure 6. Etched mirror facet is quite smooth and depth is around  $3\ \mu\text{m}$ , which is deep enough to reflect the entire mode. EBS with sub-micron gap was successfully fabricated but etched gap in EBS is too narrow to check the etch depth, sidewall slope and facet quality by visual inspection.



(a)



(b)



(c)

Figure 7. Comparison between measurement and 3D FDTD simulation: (a) normalized power transmission, (b) reflection, and (c) loss. Open symbols are the measured results and connected closed symbols are the 3D FDTD results.

Finally, BCB is spin-coated to fill the deeply-etched area and fully cured. An antireflection coating using  $\text{Ta}_2\text{O}_5$  is applied to each facet after cleaving to minimize the unnecessary reflection from cleaved facet.

The waveguides used are single mode. The measured waveguide loss is  $7 \pm 1\ \text{dB/cm}$  and  $10 \pm 1\ \text{dB/cm}$  for TE and TM modes, respectively. The main loss components are substrate leakage and the metal mask that was left on the waveguide after the fabrication. For power transmission coefficient, measured power of transmission port was normalized with that of a straight waveguide. Same procedure was done for reflection port after compensating for the loss of 2 output TIR mirrors, which is measured to be  $1 \pm 0.05\ \text{dB}$  based on a separate calibration device having the same geometry shown in Figure 6 but without the EBS. In Figure 7 (a) and (b), measured power transmission and reflection coefficients are plotted using open symbols as a function of gap dimension for different angles of incidence, respectively. They generally agree well with 3D FDTD, which are plotted with connected closed symbols, in absolute terms in addition to general trends for both power transmission and reflection data. 3D FDTD calculations predict slightly less power transmission than simulated data except for the narrower gaps. Measured power reflection match with the calculation for 0.6 and 0.7  $\mu\text{m}$  but smaller than calculation for narrower gap dimension. These deviations between 3D FDTD and data for narrow and wide gaps create differences between calculated and measured loss as shown in Figure 7 (c). There is only very good agreement between calculation and data for gaps larger than 0.5  $\mu\text{m}$ . Both non idealities in the fabrication, non vertical gap profile and insufficient gap depth, may be the reasons for deviation between measurement and 3D simulations. EBS characteristics may also show some slight wavelength dependence due to material index dispersion and corresponding change in the critical angle. But this change is within the accuracy of the experiment and we did not observe any wavelength dependent behavior within the wavelength range used in the experiments.

In summary EBS works better in waveguides with weak vertical and lateral confinement. The etched gap should have vertical sidewalls and should be almost as deep as the extent of the optical mode into the lower cladding. Angle of incidence is desired to be as high as possible. The upper limit is determined by the narrowest gap that can be etched and/or provide the required power transmission. Filling the etched trench with a high index material can be used to control the critical angle.

#### IV. CONCLUSIONS

Submicron BCB-filled etched beam splitters in weakly guiding waveguides are designed, fabricated and characterized. The measured power transmission and reflection show clear dependence on gap dimension and angle of incidence as predicted by 2D and 3D FDTD. 8 to 30% power transmission is obtained for different gap dimensions and angles of incidence. While trends agree well, the data is less than 2D simulations both in transmission and reflection. This overestimation of EBS characteristics is mainly due to not taking into account the vertical confinement in 2D simulation. More accurate

simulations using 3D FDTD show much better agreement with data. The effects of slope of the etched sidewalls and insufficient etch depth are also investigated with 3D FDTD. These results suggest sidewall slope and insufficient etch depth may be the reason for the small deviations between simulation and measurement. These observations also suggest EBS characteristics can be improved using a more weakly-guided mode in vertical direction. But this requires deeper etching which may not be easy especially for narrow gaps.

served and chaired many technical program and other professional committees. He was the Editor-in-Chief of IEEE Photonics Technology Letters 2000-2005 and an elected member of the IEEE-LEOS Board of Governors 2003-2005. He is a Fellow of IEEE.

#### REFERENCES

- [1] Y. Chung and N. Dagli, "Experimental and Theoretical Study of Turning Mirrors and Beam Splitters with Optimized Waveguide Structures," *Optical and Quantum Electronics*, vol. 27, pp. 395-403, 1995.
- [2] Jaime Cardenas, Lixia Li, Seunghyun Kim, and Gregory P. Nordin, "Compact low loss single air interface bends in polymer waveguides," *Optics Express*, Vol. 12, No. 22, November, 2004.
- [3] Doo Gun Kim, Cem Ozturk, Jae Hyuk Shin, Jong Chang Yi and Nadir Dagli, "Self-aligned total internal reflection mirrors with very low loss," *Conference Proceedings. IPR*, paper IThG5, 2004.
- [4] D. G. Kim, J. H. Shin, C. Ozturk, J. C. Yi, Y. Chung, and N. Dagli, "Total internal reflection mirror based ring resonators," *IEEE Photon. Technol. Lett.*, vol. 17, no.9, pp. 1899-1901, 2005.
- [5] H. Appelman, J. Levy, M. Pion, D. Krebs, C. Harding, and M. Zediker, "Self-aligned chemically assisted ion-beam-etched GaAs/(Al,Ga)As turning mirrors for photonic applications," *IEEE J. Lightwave Technol.*, vol. 8, pp. 39-41, 1990.
- [6] E. Gini, G. Guekos, and H. Melchior, "Low loss corner mirrors with 45° deflection angle for integrated optics," *Electron. Lett.*, vol. 28, pp. 164-175, 1992.
- [7] Wiechmann, H. J. Heider, and J. Muller, "Analysis and design of integrated optical mirrors in planar waveguide technology," *IEEE J. Lightwave Technol.*, vol. 21, pp. 1584-91, 2003.
- [8] Y. Z. Tang, W. H. Wang, T. Li and Y. L. Wang, "Integrated Waveguide Turning Mirror in Silicon-on-Insulator," *IEEE Photon. Technol. Lett.*, Vol.14, pp68-70, 2002.
- [9] B. Kim and N. Dagli, "Compact Micro Resonators with Etched Beam Splitters and Total Internal Reflection Mirrors," *Conference Proceedings. IPRA 2006*, paper IWB3, April 2006.
- [10] B. Kim and N. Dagli, "Compact Ring Resonators using Conventional Waveguides, Etched Beam Splitters and Total Internal Reflection Mirrors," *Conference Proceedings. OFC2009*, paper OWV6, March 2009.
- [11] Byungchae Kim, Yu-Chia Chang and Nadir Dagli, "Compact Add/Drop Filters Using Etched Beam Splitter and Total Internal Reflection Mirrors," *Conference Proceedings. IPNRA2009*, paper IMD6, July 2009.
- [12] Nazli Rahmadian, Seunghyun Kim, Yongbin Lin, and Gregory P. Nordin, "Air-trench splitters for ultra-compact ring resonator in low refractive index contrast waveguides," *Optics Express*, Vol. 16, No. 1, 2008.

**ByungChae Kim** (M'02) was born in Busan, Korea. He received the B.S. and M.S. degrees in electronic engineering from Pusan National University, Busan, Korea, in 2000 and 2002, respectively, and is currently working toward the Ph.D. degree in electrical engineering from the University of California at Santa Barbara, Santa Barbara. His research interests include the design, simulation, fabrication and analysis of compact resonator for optical integrated circuits.



**Nadir Dagli** received the Ph.D. degree in electrical engineering from MIT in 1986. After graduation he joined the electrical and computer engineering department at University of California at Santa Barbara, where he is currently a Professor. His current interests are design, fabrication and modeling of guided-wave components for optical integrated circuits, ultrafast electro-optic modulators, WDM components and photonic nanostructures. He